BMC Molecular and Cell Biology

RESEARCH

Open Access

RBM39 upregulation promotes ostium re-obstruction after endoscopic endonasal dacryocystorhinostomy (En-DCR)

Jinjie Liu[1†], Jinzhi Zhao[1†], Xiaoyu Zhu[1†], Xun Liu[1], Limin Zhu[1*†] and Tingting Lin[1*†]

Abstract

Purpose Chronic dacryocystitis, characterized by epiphora, is primarily treated with dacryocystorhinostomy (DCR), yet postoperative anastomotic re-obstruction remains a significant cause of failure. This study aimed to identify the key molecular mechanisms driving this recurrence.

Methods Nasal mucosal tissues were collected from 30 post-DCR patients: 15 with re-obstruction (proliferation group) and 15 with successful outcomes (non-proliferation group). Proteomic analysis based on LC-MS/MS was conducted, with differentially expressed proteins (DEPs) defined by a fold change ≥ 1.5 and $p < 0.05$. Western blot and immunohistochemistry were used for validation and localization. The role of RBM39 in vascular endothelial cell proliferation was assessed via functional experiments, and its associated pathway was analyzed.

Results Proteomics identified RBM39 as significantly upregulated in re-obstruction tissues, confirmed to be expressed in the vascular endothelium. In vitro, RBM39 overexpression enhanced HMEC-1 proliferation, while its knockdown suppressed it. KEGG pathway analysis suggested the Focal Adhesion pathway may be involved as a potential downstream mechanism.

Conclusion This study observes that RBM39 is upregulated at the anastomotic site and correlates with enhanced vascular endothelial cell proliferation. The Focal Adhesion pathway may be implicated in this process, suggesting RBM39 as a candidate target for mitigating postoperative ostium re-obstruction after En-DCR. However, further mechanistic studies are needed to establish a direct causal relationship and evaluate its therapeutic potential.

Keywords Endoscopic dacryocystorhinostomy, Proteomics, Anastomotic re-obstruction, RBM39

[†]Limin Zhu and Tingting Lin contributed equally to this work.

[†]Jinjie Liu, Jinzhi Zhao and Xiaoyu Zhu contributed equally to this work.

*Correspondence:
Limin Zhu
zlmjojo@126.com
Tingting Lin
ltt6123@126.com
[1]Tianjin Key Laboratory of Retinal Functions and Diseases, Tianjin Branch of National Clinical Research Center for Ocular Disease, Eye Institute and School of Optometry, Tianjin Medical University Eye Hospital, Tianjin, China

Introduction

Persistent epiphora, mucopurulent discharge, swelling at the medial canthus, and regurgitation on pressure characterize chronic dacryocystitis, a common lacrimal duct system disease [1, 2]. Treatment for chronic dacryocystitis aims to relieve obstruction, eliminate chronic infection, and restore normal tear drainage. The primary treatment for chronic dacryocystitis involves surgery, specifically external or endoscopic dacryocystorhinostomy (Ex-DCR or En-DCR). En-DCR has gained popularity recently because this approach offers advantages over Ex-DCR, including direct visibility of nasal anatomy, absence of visible scarring, and preservation of the medial canthal tendon to sustain the lacrimal pump mechanism. While En-DCR holds a high success rate, recurrence still affects 3% of patients through complicated etiological mechanisms that impact treatment effects and life quality. Synechiae formation in the nasal ostium represents the major cause of En-DCR surgery failure. Studies have proven that anti-fibrotic drugs, such as Mitomycin C, increase the success rate of endonasal DCR for patients with poor prognosis. Clinicians consider age, time of disease onset, systemic disease history, and nasal cavity disease history as risk factors for poor prognosis following DCR surgery. Nevertheless, some patients in clinical practice experience postoperative anastomotic obstruction without apparent causes, leaving the etiology unclear. Predicting poor prognosis after DCR surgery from a molecular biology perspective is therefore particularly important.

In 1996, Wilkins et al. [3] defined proteomics as the extensive research of the full set of proteins found in a cell, tissue sample, or organism. The field comprises protein expression levels, 3D structures, post-translational modifications, and protein-protein interactions. Such data offers a comprehensive understanding of cell function and disease pathology at the protein level. These advancements in proteomics have then facilitated broader applications of bioinformatics in lacrimal duct disease research. Discovery of potential biomarkers and development of new therapeutic strategies rely on integrating large-scale data to identify key genes involved in anastomotic re-obstruction following DCR [4]. Findings require orthogonal validation, however, due to inherent technical limitations in proteomics such as instrument accuracy and non-negligible false-positive rates. We then verified the differential protein RBM39 identified in this study at both the gene and protein levels. Our work represents the first prospective analysis globally to use proteomics for predicting poor prognosis associated with anastomotic obstruction after DCR surgery through differentially expressed proteins in nasal mucosa. This research offers a theoretical foundation for explaining underlying mechanisms and developing future interventions by combining proteomic and bioinformatic analyses to identify and verify key genes in post-DCR re-obstruction.

Tissue samples

We prospectively collected nasal mucosal tissues from patients diagnosed with chronic dacryocystitis during endoscopic dacryocystorhinostomy at Tianjin Medical University Eye Hospital between February and June 2024. Written informed consent was obtained from every patient. Nasal mucosal tissues from all patients were obtained during the primary En-DCR surgery, with the specific procedure as follows: The projection of the lacrimal sac onto the lateral nasal wall was located under nasal endoscopy. Lidocaine with epinephrine was injected submucosally at this site for hemostasis and local infiltration anesthesia. A "U"-shaped mucoperiosteal flap was created in the area of the lacrimal sac projection using a sickle knife, and a mucosal tissue specimen approximately 5 mm*5 mm in diameter was harvested from this flap. All patients were followed up at three months postoperatively, including symptom inquiry, lacrimal irrigation, and nasal endoscopy examination. Anastamosis re-obstruction was defined by the following: (1) a lack of any improvement in epiphora symptoms; (2) confirmed scarring and/or granuloma-based occlusion of the lacrimal sac ostium visible upon endonasal endoscopic examination; (3) apparent obstruction of the lacrimal system evident upon irrigation. For those patients confirmed to have anastomotic re-obstruction, we performed anastomotic revision surgery under endoscopic assistance. We assigned participants developing re-obstruction of the anastomosis to the proliferation group ($n = 15$). We selected patients with patent anastomoses as the non-proliferation group after matching for age, sex, and medical history ($n = 15$). We conducted this study in accordance with the Declaration of Helsinki principles. The Ethics Committee of Tianjin Medical University Eye Hospital granted approval (Approval No. 2024KY(L)-25).

Proteomic sample preparation and analysis

Using ProteinPilot software (v5.0.1; AB SCIEX), IDA data, reference library construction, and protein identification were analyzed using the UniProt human SwissProt database (https://www.uniprot.org/, released 2023.03). The SWATH quantitation microapp of peakView Software (v2.2, AB SCIEX) was used to the extract SWATH-MS peaks. The entire process took 12 minutes and the detailed parameters were as follows: six peptides and six transitions, shared and modified peptides excluded, peptide confidence > 99%, XIC width 50ppm, and FDR < 1%. Quantitative values were based on peak areas. Post-processing of quantitative data included log2 transformation and median normalization using the "preprocessCore"

package in R. Differential analysis was performed using the 'stats' package in R. DEPs were screened p-values < 0.05 and fold change ≥ 1.5. SPSS software (v26.0) was used to analyze statistical significance. Student's t-test was used to analyze data with normal distribution. More detailed MS parameters are included in Supplementary Notes A1.

Differential protein screening

Differential protein expression analysis was conducted using the limma package in R. Proteins were considered differentially expressed if they showed a log2-fold change greater than 1.5 and a p-value below 0.05. The 'heatmap' and 'ggplot2' R packages generated heatmaps and volcano plots.

Western blotting

Proteins were extracted by lysing tissues and cells with RIPA buffer. Proteins are separated by SDS-PAGE and incubated them overnight at 4 °C with the following primary antibodies: RBM39 (1:1200), ACTN1 (1:1500), VASP (1:600), and GAPDH (1:3000). The membranes were washed with TBST and then incubated with a secondary antibody conjugated to HRP at a 1:2000 dilution. An ECL substrate detected the protein bands.

Immunohistochemistry

Tissue sections were deparaffinised, rehydrated, and treated to inhibit endogenous peroxidase activity. Antigen retrieval was accomplished using a microwave approach under increased pressure. Standard goat serum was utilized to obstruct the sections. Then, the sections were incubated with a primary antibody directed against RBM39 at 4 °C for 12–18 h. The sections were rinsed with PBS and then exposed to a secondary antibody at 37 °C for 30 min. Staining was developed utilizing DAB, and the nuclei were counterstained. PBS replaced the primary antibody to act as a negative control. A positive control was offered by the reagent manufacturer. An experienced pathologist evaluated the stained tissue sections. RBM39 positivity was primarily localized to the vascular endothelium, as the protein was present in the endothelium of blood vessels.

Human microvascular endothelial (HMEC-1) cell culture

HMEC-1 Cell was purchased from the Stem Cell Bank of the Chinese Academy of Sciences and cultured in MCDB131 medium consisting of 10% fetal bovine serum, penicillin and streptomycin (100 μg/mL), and human epidermal growth factor (hEGF, 10 ng/mL). Cultivation of the cells occurred at 37 °C in a 5% CO_2 incubator, while the medium was replenished at intervals of 2–3 days. Experiments were carried out using cells at a concentration of 1×10^6 cells/mL during their logarithmic growth phase.

siRNA knockdown of RBM39

We seeded 6-well plates utilizing HMEC-1 cells in the logarithmic growth phase. Transfection of the cells was carried out utilizing Lipofectamine 3000 at 70% confluence, following the manufacturer's guidelines. Five μl of Lipofectamine 3000 diluted in 250 μl Opti-MEM (Solution A) was utilized for each well. We prepared both a negative control RNAi and RNAi targeting RBM39 (siRNA-RBM39) in this manner. Incubation of these mixtures lasted for five minutes. The study then combined Solution A with the siRNA mixture and incubated it at ambient temperature for 30 min. The transfection complex was added to cells in 1.5 mL of Opti-MEM medium. RT-qPCR and Western blotting verified the effectiveness of the knockdown after a 48-hour incubation period.

Lentiviral transduction for RBM39 overexpression

HMEC-1 cells were seeded in 6-well plates. Cells at 50–70% confluence were transduced with a lentivirus containing RBM39 at a multiplicity of infection of 10. The virus volume was determined by multiplying the MOI with the Cell Number and then dividing by the Viral Titer (in PFU/mL). This viral suspension was added to the cells utilizing half the volume of fresh medium. After 12–16 h, we replaced the medium containing the virus with fresh complete medium. Fluorescence microscopy evaluated the infection efficiency after 72 h, while RT-qPCR and Western blotting confirmed the expression.

Reverse transcription-quantitative PCR (RT-qPCR)

Total RNA was extracted and reverse transcribed. The cDNA synthesis was followed by quantitative PCR using SYBR-Green. A real-time PCR system was used to perform the PCR. The RBM39 mRNA expression was calculated utilizing the $2^{\wedge -\Delta\Delta CT}$ method with GAPDH as the internal standard.

Cell proliferation assay (CCK-8)

A 100 μL droplet of HMEC-1 cells was placed into 96-well plates and allowed to sit for 24 h. The medium was replaced with an equal volume of fresh medium comprising, and the plates were incubated for a further 24 h. Afterward, 10 μL of CCK-8 reagent was added to each well, and the plates were left to incubate for a further 2–4 h. A microplate reader measured the absorbance at 450 nm.

Enzyme-linked immunosorbent assay (ELISA)

The VEGF levels in the cell culture media were measured with a human VEGF ELISA kit. Samples and standards were added to the pre-coated plate before incubation

with a biotinylated detection antibody and HRP-streptavidin. After completing the washing step, a substrate solution was added, and the reaction was terminated at this stage. A microplate reader (LianKe, RT-6100) measured the 450 nm absorption.

Statistical analysis

Statistical analyses were conducted using SPSS version 23 and GraphPad Prism version 9. The Shapiro–Wilk test verified that the data followed a normal distribution. Differences between two groups were examined using an independent samples t-test. A one-way ANOVA was conducted, followed by an LSD post hoc test, to compare multiple groups. A p-value of less than 0.05 was deemed statistically significant.

Results

Differential protein screening in patient tissues

We obtained nasal mucosal tissues from 30 patients with chronic dacryocystitis. This cohort comprised a proliferation group ($n = 15$) of patients with postoperative anastomotic re-obstruction and a non-proliferation control group ($n = 15$) of patients post-DCR patent ostium. 8 samples are subjected to LC-MS/MS -based proteomic analysis.

Quality control indicated high data reproducibility, as evidenced by Pearson correlation coefficients of 0.83 or higher in and between groups (Fig. 1A). Principal Component Analysis plot demonstrated high intra-group consistency and clear inter-group separation, confirming the robustness and statistical reliability of the data (Fig. 1B). We analyzed a total of 3,056 proteins and identified 51 DEPs between the proliferation and control groups. This total included 26 upregulated and 25 downregulated

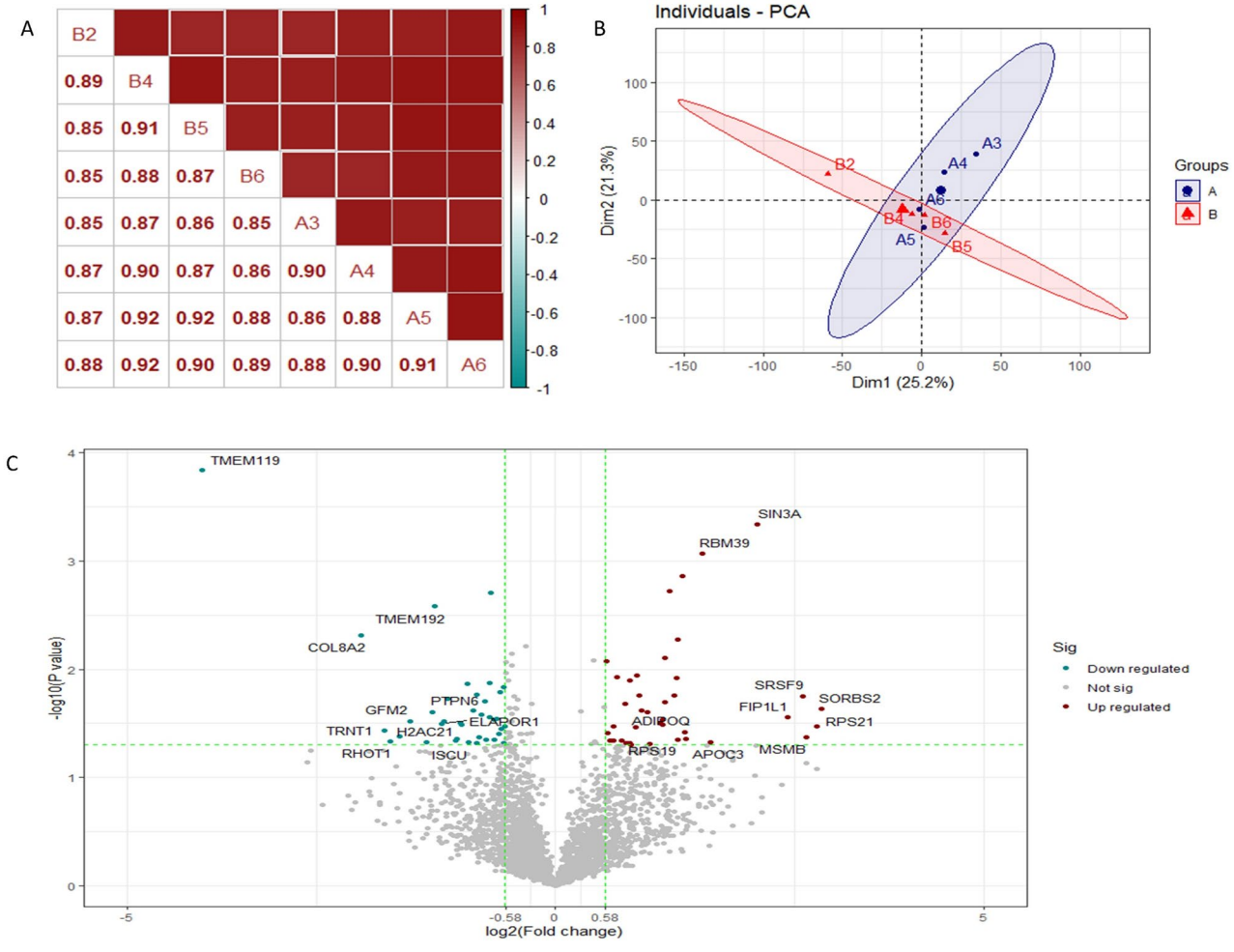

Fig. 1 Quality control of the proteomic analysis. (**A**) Pearson's correlation coefficients representing correlations between samples. A higher correlation and deeper red color indicate higher data reproducibility, while the color bar ranges from red (high correlation) to green (low correlation). (**B**) Principal Component Analysis plot. The more samples in the group, the better the reproducibility within the group, and the more obvious the separation between different groups, indicating that the difference between groups is more significant. (**C**) Volcano plots illustrating overall protein differences

proteins (Fig. 1B). SORBS2, RSP21, APOC3, SIN3A, FIP1L1, SRSF9, and RBM39 were among the significantly upregulated proteins; whereas, TMEM119, COL8A2, TRNT1, RHOT1, H2AC21, GFM2, and ISCU appeared significantly downregulated (Fig. 1C).

Analysis utilizing Gene Ontology (GO) indicated that these DEPs primarily localized to sites of focal adhesion and RNA catabolism (Fig. 2A). Besides, KEGG pathway enrichment analysis indicated significant involvement in the PPAR signaling pathway and RNA metabolism, among others (Fig. 2B). We utilized a clustering heatmap to confirm consistent DEP expression patterns in groups, which further supported sample reproducibility (Fig. S1). We selected RBM39 for further validation due to its established role in regulating microvascular density and vascular endothelial expression. These are key factors in chronic inflammation and wound healing.

Validation of RBM39 expression in human nasal mucosal tissue

Results from immunohistochemistry confirmed that RBM39 prominently localized to the vascular endothelium of nasal mucosal tissue (Fig. 3A). Further analysis through the Western blot method indicated that RBM39 protein expression was noticeably greater in the PG compared to the NPG (Fig. 3B, C).

Effect of RBM39 on HMEC-1 cell proliferation, migration, and VEGF expression

Successful knockdown and overexpression of RBM39

HMEC-1 cells transfected with siRNAs exhibited significantly lower levels of RBM39 mRNA and protein relative to the control group (Fig. 4A–C). Through lentiviral transduction, we established a cell line that overexpresses RBM39, resulting in notably higher mRNA and protein expression than the control group with an empty plasmid (Fig. 4D–F).

RBM39 modulates cell proliferation and migration

Results from CCK-8 assays conducted 72 h post-transfection indicated that cell viability (A value) decreased in the RBM39-knockdown group but increased in the RBM39-overexpression group relative to their respective controls (Fig. 4I). Besides, wound healing assays indicated that RBM39 knockdown impaired cell migration, whereas RBM39 overexpression enhanced this process (Fig. 4G, H).

RBM39 alters VEGF expression

ELISA analysis of the cell culture supernatant revealed a significant increase in VEGF levels in the RBM39-overexpressing group. However, no significant difference in VEGF expression levels was observed between the

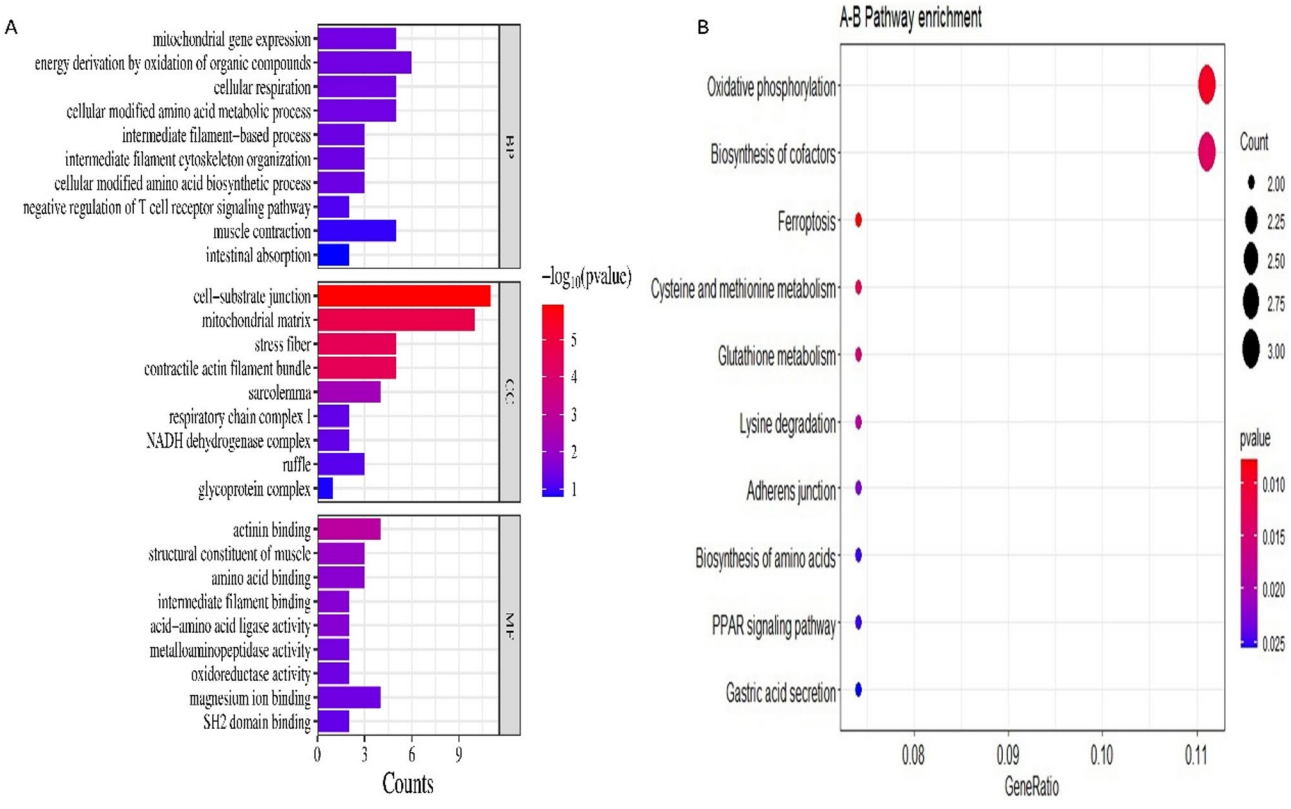

Fig. 2 Bioinformatics analysis (**A**) GO enrichment analysis of differentially expressed proteins (DEPs). (**B**) KEGG pathway enrichment analysis of DEPs

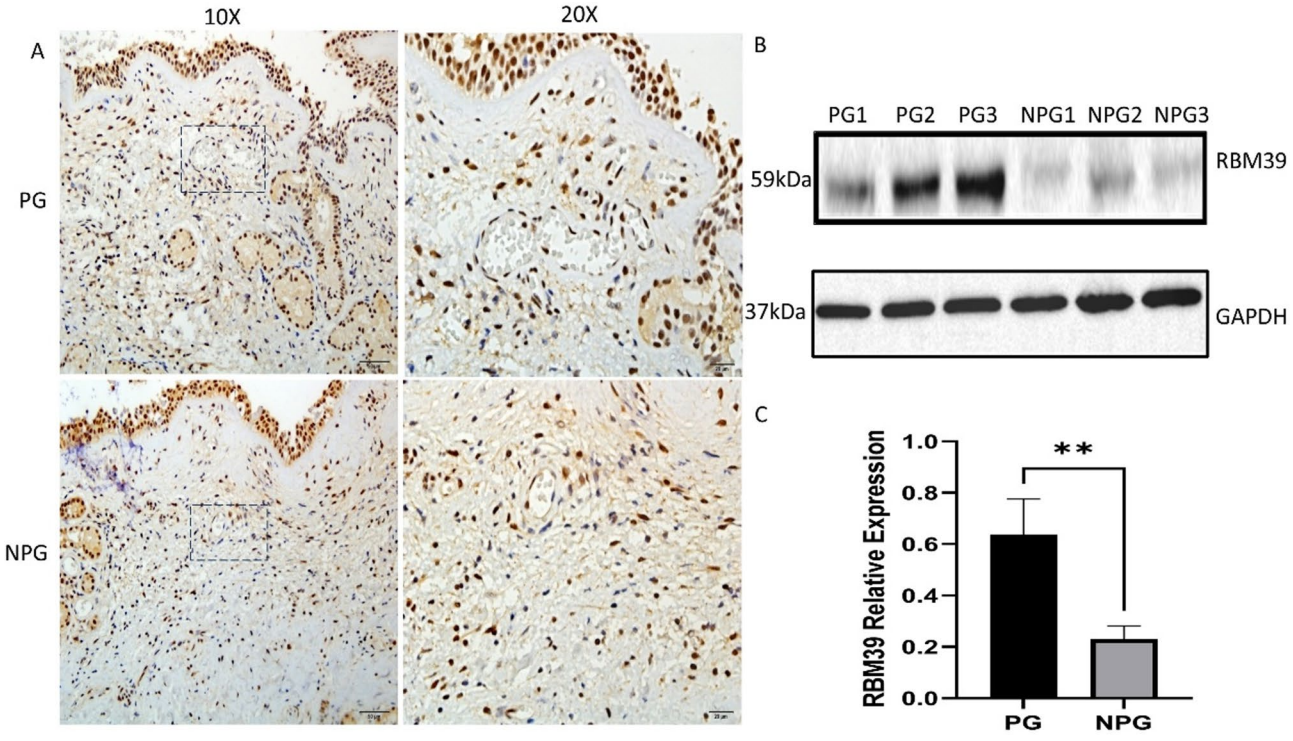

Fig. 3 RBM39 is over expressed in recurrent nasal mucosal tissue. (**A**) Immunohistochemistry of nasal mucosal tissue in the proliferation (recurrent) group and the non-proliferation (control) group. (**B, C**) Western blotting results and quantitative analysis (WB data are presented as the mean percentage of NC group ± SD ($n = 3$, each measured in triplicate. Statistical significance was determined by an unpaired two-tailed Student's t-test; *$P<0.05$,**$P<0.01$,***$P<0.001$,****$P<0.0001$.)

RBM39-knockdown group and the control group. These findings suggest that RBM39 may participate in influencing the biological functions of endothelial cells by regulating VEGF expression, but its specific regulatory mechanism may be compensated by other factors under low-expression conditions (Fig. 4J).

Proteomic analysis of HMEC-1 cells with altered RBM39 expression

We observed high data quality during the proteomic profiling of RBM39-knockdown (KD) and overexpressing (OE) HMEC-1 cells against their controls (NC) (Pearson's $r \geq 0.87$; Fig. 5A). Principal Component Analysis plot demonstrated high intra-group consistency and clear inter-group separation, confirming the robustness and statistical reliability of the data (Fig. 5B). The KD-NC comparison derived 165 DEPs (96 upregulated, 69 downregulated), while the OE-NC comparison indicated 409 DEPs (167 upregulated, 242 downregulated) (Fig. 5C). In addition, clustering heatmaps verified the strong reproducibility associated with these proteomic profiles (Fig. S2,3).

Bioinformatics analysis and protein-protein interaction (PPI) network

Our analysis of the proteomic data from the RBM39-overexpression experiment aimed to explain the role of RBM39 in anastomotic occlusion. Analysis of GO enrichment indicated significant involvement of DEPs in biological processes (BPs), cellular components (CCs), and molecular functions (MFs). Besides, KEGG pathway analysis highlighted enrichment in spliceosomes, ribosomes, the HIF-1 signaling pathway, and focal adhesion (Fig. 6B). We utilized the STRING database to construct a PPI network that displays interactions between RBM39 and other DEPs (Fig. 6D). We selected ACTN1 (alpha-actinin-1) and VASP (vasodilator-stimulated phosphoprotein) as key downstream proteins and the focal adhesion pathway for further analysis after comprehensively studying the DEPs, GO, and KEGG results (Fig. 6E).

Western blot validation of the focal adhesion pathway

We conducted Western blot analysis to offer validation for the bioinformatics findings. This process involved comparing the expression levels of key focal adhesion pathway proteins, including ACTN1, VASP, and Akt, between RBM39-overexpressing HMEC-1 cells and control cells. The results showed that the expression of

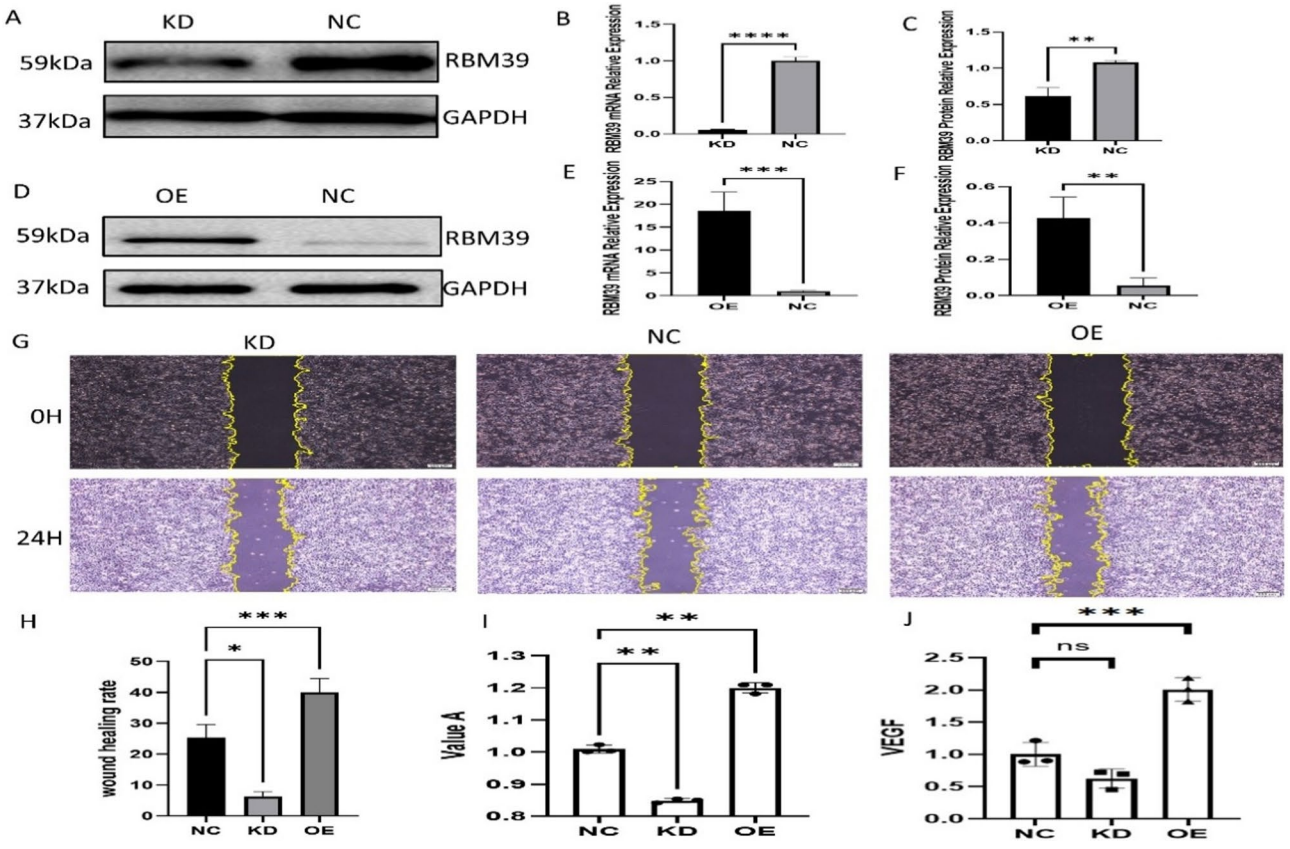

Fig. 4 Proliferation, migration, and cell supernatant VEGF expression of HMEC-1 Cell under knockdown and overexpression of RBM39. (**A–C**) Validation of knockdown efficiency via Western blot and PCR. (**D–F**) Validation of overexpression efficiency through Western blot and PCR. (**G**) Representative images of cell migration from the wound healing assay. (**H**) Quantitative analysis of the wound healing assay following RBM39 knockdown and overexpression. (**I**) CCK-8 assay analysis of cell viability following RBM39 knockdown and overexpression. Wound healing data are presented as the mean percentage of NC group ± SD ($n = 3$, each measured in triplicate. Statistical significance was determined by one-way ANOVA test; *$P<0.05$,**$P<0.01$,***$P < 0.001$,****$P<0.0001$). There are 9 images per group in each time period. (**J**) ELISA analysis of VEGF levels in cell supernatants following RBM39 knockdown and overexpression.ELISA data are presented as the mean percentage of NC group ± SD ($n = 3$, each measured in triplicate. Statistical significance was determined by one-way ANOVA test; *$P<0.05$,**$P<0.01$,*** $P < 0.001$,****$P<0.0001$.)

ACTN1 in the RBM39 overexpression group was significantly down-regulated, and the expression of VASP and Akt proteins was significantly up-regulated, which was consistent with the results of proteomics (Fig. 6F).

Discussion

This study represents, to our knowledge, the first prospective proteomic analysis aimed at identifying molecular determinants of postoperative ostium re-obstruction following En-DCR. By comparing the nasal mucosal proteomes of patients with successful surgical outcomes versus those who developed re-obstruction, we identified RNA-binding motif protein 39 (RBM39) as a significantly upregulated protein in the proliferation group. Immunohistochemistry confirmed its predominant localization to the vascular endothelium, suggesting a potential role in angiogenic processes. Through a series of in vitro functional experiments in HMEC-1 cells, we demonstrated that RBM39 promotes endothelial cell proliferation, migration, and VEGF secretion, while its knockdown exerts opposite effects. Mechanistically, integrated bioinformatic and proteomic analyses of RBM39-manipulated cells implicated the focal adhesion signaling pathway as a key downstream mediator, a finding further supported by Western blot validation of ACTN1, VASP, and Akt expression. Collectively, our findings position RBM39 as a novel molecular player in postoperative scar formation and identify it as a potential therapeutic target for preventing surgical failure after En-DCR.

The pathogenesis of re-obstruction after DCR is multifactorial, with excessive scarring and synechiae formation at the nasal ostium being the predominant causes of surgical failure [5, 6]. While clinical factors such as age, diabetes, prior sinus surgery, and chronic inflammation are known to influence outcomes [6], the underlying molecular mechanisms driving aberrant wound healing remain poorly defined. Our study addresses this critical gap by providing a comprehensive proteomic landscape

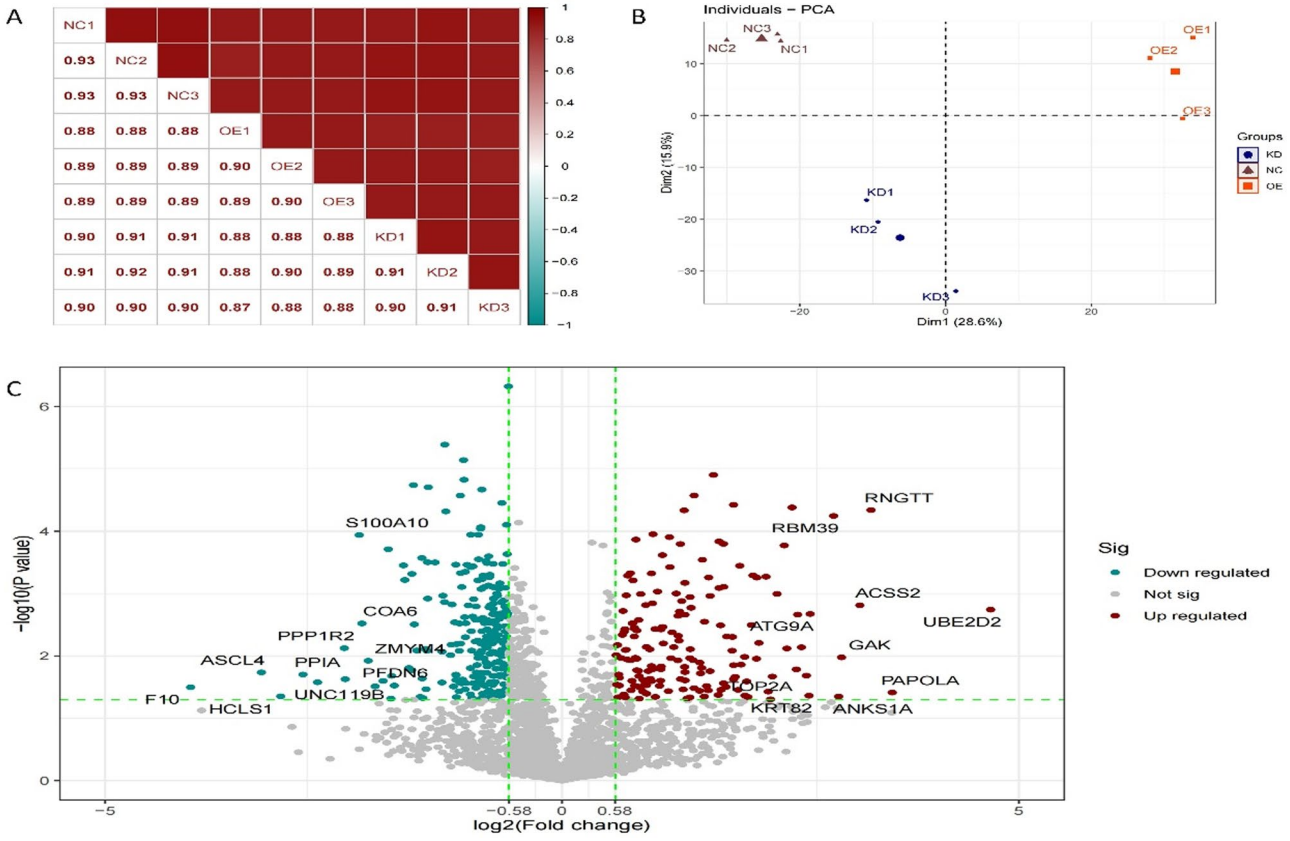

Fig. 5 Quality control of the proteomic analysis. (**A**) Pearson's correlation coefficients representing correlations between samples. Deeper red indicates higher correlation and data reproducibility; the color scale ranges from red (high) to green (low). (**B**) Principal Component Analysis plot. The more samples in the group, the better the reproducibility within the group, and the more obvious the separation between different groups, indicating that the difference between groups is more significant. (**C**) Volcano plots illustrating overall protein differences

of the nasal mucosa at the anastomotic site. The identification of 51 differentially expressed proteins between the proliferation and non-proliferation groups—including upregulation of RBM39, SORBS2, and SRSF9—highlights the intricate molecular remodeling associated with failed surgical outcomes. Notably, Gene Ontology enrichment analysis revealed that these differentially expressed proteins are significantly enriched in focal adhesion and RNA catabolism pathways, suggesting that both structural dynamics and post-transcriptional regulation contribute to the pathological processes leading to ostial occlusion.

RBM39, also known as HCC1 or CAPERα, is a member of the serine/arginine-rich family of RNA-binding proteins involved in alternative splicing and transcriptional co-regulation [7]. Its role in cancer biology has been increasingly recognized, particularly in regulating angiogenesis and tumor progression [8–10]. RBM39 has been shown to modulate the expression of angiogenic factors and to influence endothelial cell behavior in tumor microenvironments. However, its function in benign fibroproliferative disorders such as post-surgical scarring has not been previously explored. Our observation that RBM39 is upregulated in restenotic nasal mucosal tissues and localized to the vascular endothelium provides a critical link between its known angiogenic functions and the pathology of postoperative re-obstruction.

Angiogenesis is a fundamental component of normal wound healing, providing oxygen and nutrients to regenerating tissues [11, 12]. However, when dysregulated, excessive angiogenesis can contribute to the formation of hyperplastic granulation tissue, which serves as a scaffold for fibrotic scar formation. This process is well documented in other fibrotic diseases and in the context of surgical failure following sinus surgery [13, 14]. In the setting of DCR, excessive granulation tissue at the anastomotic site can lead to ostial stenosis and functional failure. The upregulation of RBM39 in patients with re-obstruction suggests that it may drive an aberrant pro-angiogenic response, tipping the balance from normal wound healing toward pathological scarring.

Our in vitro experiments using HMEC-1 cells provide direct functional evidence supporting this hypothesis. RBM39 overexpression significantly enhanced endothelial cell proliferation and migration, two key processes in angiogenesis, while RBM39 knockdown suppressed

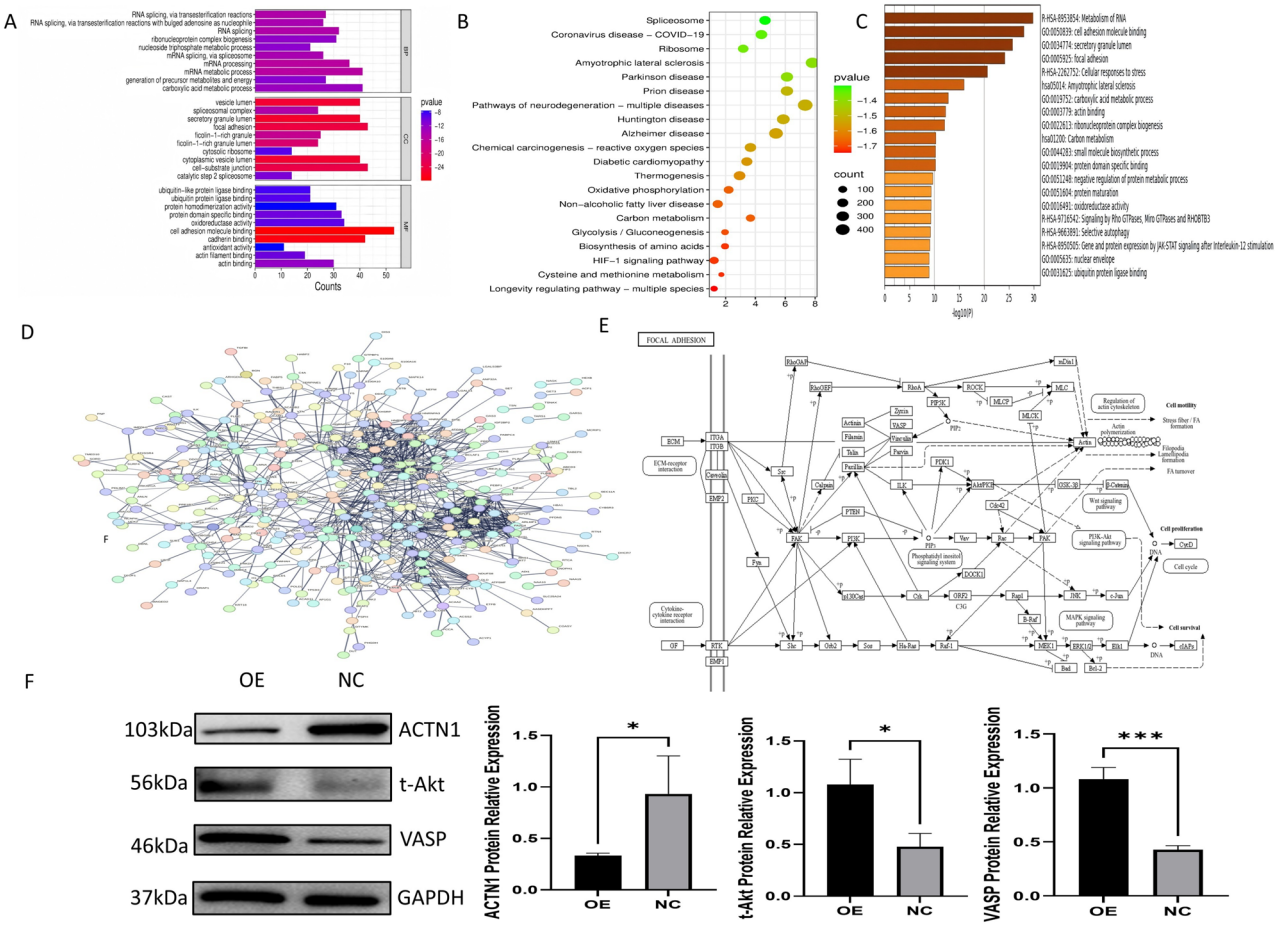

Fig. 6 Association of RBM39 with the focal adhesion pathway (**A**) GO enrichment analysis of differentially expressed proteins. (**B**) KEGG pathway enrichment analysis. (**C**) Bar chart indicating the top 20 functional terms determined using Metascape (GO, KEGG, and Reactome). (**D**) Protein-protein interaction (PPI) network construction. (**E**) Diagram of the KEGG focal adhesion pathway. (**F**) Western blotting results and quantitative analysis of proteins in the focal adhesion pathway.WB data are presented as the mean percentage of NC group ± SD ($n = 3$, each measured in triplicate). Statistical significance was determined by an unpaired two-tailed Student's t-test; *$P<0.05$,**$P<0.01$,*** $P<0.001$,****$P<0.0001$

these cellular behaviors. Furthermore, we observed that RBM39 overexpression led to a significant increase in VEGF secretion, whereas knockdown did not produce a statistically significant decrease. This asymmetric response may reflect the presence of compensatory mechanisms or the fact that basal VEGF expression is maintained by multiple regulatory pathways. Nevertheless, the increase in VEGF upon RBM39 overexpression suggests that it can potentiate a pro-angiogenic milieu, which in vivo would likely promote granulation tissue formation and scar deposition.

To elucidate the downstream signaling pathways mediating these effects, proteomic profiling of HMEC-1 cells was performed with variations in RBM39 expression. The differentially expressed proteins identified in these cells were subjected to pathway enrichment analysis, which highlighted the focal adhesion pathway as a significantly enriched category. Focal adhesions are macromolecular complexes that link the extracellular matrix to the intracellular actin cytoskeleton and serve as critical hubs for mechanotransduction, cell adhesion, migration, proliferation, and survival [15–17]. In fibrotic diseases, dysregulation of focal adhesion signaling contributes to the activation and persistence of myofibroblasts, as well as to excessive extracellular matrix deposition [18, 19]. Our Western blot validation confirmed that RBM39 overexpression in HMEC-1 cells upregulates ACTN1 and VASP, both of which are integral components of the focal adhesion complex. ACTN1 functions as an actin-crosslinking protein that stabilizes focal adhesions and promotes cell motility [20–22], while VASP is involved in actin polymerization and is essential for directional cell migration [23–25]. The coordinated upregulation of these proteins suggests that RBM39 may enhance the migratory capacity of endothelial cells by strengthening focal adhesion dynamics, thereby facilitating the cellular processes required for neovascularization and granulation tissue formation. Additionally, the observed increase in Akt

expression, a central node in growth factor and survival signaling, further supports the notion that RBM39 promotes a pro-proliferative and pro-survival phenotype in endothelial cells.

Existing studies related to postoperative nasal wound repair have mainly focused on classic pro-fibrotic and pro-angiogenic mediators, such as TGF-β, VEGF, and various inflammatory cytokines, which are generally regarded as common biomarkers linked to aberrant wound healing processes. Most of these reported molecules only act as passive phenotypic indicators that correlate with the severity of abnormal tissue repair, rather than functioning as core upstream regulators coordinating the overall pathological process. In addition, previous transcriptomic and proteomic investigations on DCR restenosis have largely concentrated on differentially expressed structural proteins and inflammatory factors, while few studies have identified promising upstream regulatory molecules with prospective intervention potential.

Compared with these commonly reported markers associated with tissue repair and vascular remodeling, our findings suggest that RBM39 is far more than a routine diagnostic biomarker. As an RNA-binding protein participating in alternative splicing and transcriptional modulation, RBM39 may serve as a vital upstream regulator that modulates endothelial biological phenotypes and the downstream focal adhesion signaling network at both transcriptional and post-transcriptional levels. RBM39 is likely to participate in regulating endothelial proliferation and migration. In this regard, RBM39 emerges as a potential upstream intervention node in the pathological cascade of postoperative ostial re-obstruction, offering a promising candidate distinct from conventional passive biomarkers for future exploratory targeted strategies. Targeting RBM39 may help modulate dysregulated endothelial behavior and abnormal wound healing, which could provide a novel research direction for improving long-term En-DCR outcomes, unlike the relatively single regulatory effect of traditional markers such as VEGF.

Several limitations of this study warrant consideration. First, multiple-testing correction was not performed for differential protein statistical analysis, and differentially expressed proteins were screened merely based on raw P-values and fold-change without effect size evaluation. This may bring potential false-positive results caused by multiple statistical comparisons. Besides, the sample size is relatively limited, and the findings need to be further validated in larger independent cohorts and mechanistic experiments. Second, our in vitro experiments were conducted using a single HMEC-1 cell line. While this model is well-established for studying endothelial function, the nasal mucosal microenvironment comprises a complex interplay among endothelial cells, fibroblasts, inflammatory cells, and epithelial cells. Future work should incorporate co-culture systems (e.g., endothelial-fibroblast) to validate these findings in a more physiologically relevant context. Third, while our data demonstrate that RBM39 upregulation correlates with enhanced endothelial cell proliferation, migration, and VEGF secretion, the current evidence remains primarily correlative. Although RBM39 is known to regulate alternative splicing and RNA stability as an RNA-binding protein, we have not established direct mechanistic links between RBM39 and focal adhesion pathway activation. Specifically, no experimental evidence (e.g., pathway inhibition assays, transcriptional target validation, or splicing pattern analyses) currently supports RBM39's direct modulation of focal adhesion components such as ACTN1 or VASP. Finally, while our findings suggest RBM39 may play a role in angiogenesis relevant to wound healing and DCR, the current study does not provide direct evidence for its therapeutic targeting potential. Future investigations using in vivo models of pathological scarring—such as a rabbit lacrimal surgery model—will be critical to evaluate.

Despite these limitations, our study has several important strengths. The prospective collection of well-characterized human nasal mucosal tissues from patients undergoing En-DCR with clearly defined clinical outcomes provides a clinically relevant and robust discovery platform. The integration of unbiased proteomics with functional cellular assays and pathway validation represents a powerful approach for identifying key molecular drivers of surgical failure. The identification of RBM39 as a novel player in postoperative scarring not only expands our understanding of the pathophysiology of re-obstruction but also opens new avenues for therapeutic intervention.

Conclusion

In summary, the results of this study support the hypothesis that RBM39 could contribute to anastomotic re-obstruction after En-DCR surgery. Our data suggest RBM39 may influence endothelial cell proliferation, migration, and VEGF secretion, potentially via modulation of the focal adhesion pathway. These observations highlight RBM39 as a candidate biomarker and therapeutic target for mitigating surgical failure. However, further mechanistic studies are needed to clarify the direct role of RBM39 in fibrotic processes and to evaluate the translational potential of targeting RBM39 or its downstream effectors. Such efforts could inform new strategies for improving long-term outcomes in DCR and other surgeries complicated by excessive scarring.

Abbreviations

En-DCR	Endoscopic Endonasal Dacryocystorhinostomy
PG	Proliferation Group

NPG	Not Proliferation Group
DEP	Differentially Expressed Proteins
DEG	Differentially Expressed Genes
GO	Gene Ontology
KEGG	Kyoto Encyclopedia of Genes and Genomes
IHC	Immunohistochemistry
WB	Western Blotting
qPCR	Quantitative Real-time PCR
siRNA	Small Interfering RNA
KD	Knock Down
OE	Over Expression
CCK-8	Cell Counting Kit-8
Elisa	Enzyme-Linked Immunosorbent Assay

Supplementary Information

The online version contains supplementary material available at https://doi.org/10.1186/s12860-026-00596-6.

Supplementary Material 1

Supplementary Material 2

Supplementary Material 3

Supplementary Material 4

Supplementary Material 5

Supplementary Material 6

Supplementary Material 7

Supplementary Material 8

Supplementary Material 9

Author contributions

The authors confirm contribution to the paper as follows: Validation Analysis and interpretation of results: Jinjie Liu; Conception and design of study: Jinzhi Zhao and Xun Liu; Data collection: Xiaoyu Zhu; Drafting the manuscript: Jinzhi Zhao and Jinjie Liu; All authors reviewed the results and approved the final version of the manuscript.

Funding

This study was funded by Tianjin Key Medical Discipline Construction Project (TJYXZDXK-3-004A-2), Independent project of Tianjin Key Laboratory of retinal function and disease(2021tjswmq003) and the Science&Technology Development Fund of Tianjin Education Commission for Higher Education (2025ZD019 and 2025KJ030).

Data availability

The datasets used and/or analysed during the current study are available from the corresponding author on reasonable request.

Declarations

Ethics approval and consent to participate

The authors confirm that any aspect of the work covered in this manuscript that involved human patients or animals was conducted with the ethical approval of all relevant bodies and the study was performed in accordance with the Declaration of Helsinki, and the protocol was approved by the Ethics Committee of Tianjin Medical University Eye Hospital [Approval No.: 2024KY(L)-25]. All participants were fully informed of the study procedures, potential risks, and rights prior to enrollment. Written informed consent was obtained from all participants before sample collection and data usage.

Consent for publication

Not applicable. This study does not contain any individual person's identifiable data or images requiring consent for publication.

Competing interests

The authors declare no competing interests.

Received: 26 January 2026 / Accepted: 21 May 2026
Published online: 09 June 2026

References

1. Janssen AG, Mansour K, Bos JJ, Castelijns JA. Diameter of the bony lacrimal canal: normal values and values related to nasolacrimal duct obstruction: assessment with CT. AJNR Am J Neuroradiol. 2001;22(5):845–50.
2. Chin J, Lam V, Chan R, Li CL, Yeung L, Law A, Young A, Yuen H, Ali MJ, Chong KKL. Comparative study of stenting and ostium packing in endoscopic dacryocystorhinostomy for primary acquired nasolacrimal duct obstruction. Sci Rep. 2020;10:46(1).
3. Wilkins MR, Sanchez JC, Gooley AA, Appel RD, Humphery-Smith I, Hochstrasser DF, Williams KL. Progress with proteome projects: why all proteins expressed by a genome should be identified and how to do it. Biotechnol Genet Eng Rev. 1996;13:19–50.
4. Yang Q, Feng M, Ma X, Li H, Xie W. Gene expression profile comparison between colorectal cancer and adjacent normal tissues. Oncol Lett. 2017;14(5):6071–8.
5. Choi JC, Jin HR, Moon YE, Kim MS, Oh JK, Kim HA, Choi MY, Shim WS. The surgical outcome of endoscopic dacryocystorhinostomy according to the obstruction levels of lacrimal drainage system. Clin Exp Otorhinolaryngol. 2009;2(3):141–4.
6. Liu S, Zhang H, Zhang YR, Chen LJ, Yu XY. The efficacy of endoscopic dacryocystorhinostomy in the treatment of dacryocystitis: A systematic review and meta-analysis. Med (Baltim). 2024;103(11):e37312.
7. Xu Y, Nijhuis A, Keun HC. RNA-binding motif protein 39 (RBM39): An emerging cancer target. Br J Pharmacol. 2022;179(12):2795–812.
8. Wang Y, Yang X, Yang Z, Chen Z, Jiang H, Wang Y, Shen D, Su G. RBM39 Functions as a Potential Oncogene Through the NF-κB Signaling Pathway in Colorectal Cancer Cells. J Cancer. 2025;16(7):2233–49.
9. Xu C, Chen X, Zhang X, Zhao D, Dou Z, Xie X, Li H, Yang H, Li Q, Zhang H, et al. RNA-binding protein 39: a promising therapeutic target for cancer. Cell Death Discov. 2021;7(1):214.
10. Jang JH, Kim JY, Lee TJ. Recent advances in anticancer mechanisms of molecular glue degraders: focus on RBM39-dgrading synthetic sulfonamide such as indisulam, E7820, tasisulam, and chloroquinoxaline sulfonamide. Genes Genomics. 2024;46(12):1345–61.
11. Shi Z, Yao C, Shui Y, Li S, Yan H. Research progress on the mechanism of angiogenesis in wound repair and regeneration. Front Physiol. 2023;14:1284981.
12. Eming SA, Martin P, Tomic-Canic M. Wound repair and regeneration: mechanisms, signaling, and translation. Sci Transl Med. 2014;6(265):265sr266.
13. Stone RC, Chen V, Burgess J, Pannu S, Tomic-Canic M. Genomics of human fibrotic diseases: disordered wound healing response. Int J Mol Sci. 2020;21(22).
14. Arif S, Attiogbe E, Moulin VJ. Granulation tissue myofibroblasts during normal and pathological skin healing: The interaction between their secretome and the microenvironment. Wound Repair Regen. 2021;29(4):563–72.
15. Kuo JC. Mechanotransduction at focal adhesions: integrating cytoskeletal mechanics in migrating cells. J Cell Mol Med. 2013;17(6):704–12.
16. Provenzano PP, Keely PJ. Mechanical signaling through the cytoskeleton regulates cell proliferation by coordinated focal adhesion and Rho GTPase signaling. J Cell Sci. 2011;124(Pt 8):1195–205.
17. Kanchanawong P, Calderwood DA. Organization, dynamics and mechanoregulation of integrin-mediated cell-ECM adhesions. Nat Rev Mol Cell Biol. 2023;24(2):142–61.
18. Hinz B, Lagares D. Evasion of apoptosis by myofibroblasts: a hallmark of fibrotic diseases. Nat Rev Rheumatol. 2020;16(1):11–31.
19. Kramann R, DiRocco DP, Humphreys BD. Understanding the origin, activation and regulation of matrix-producing myofibroblasts for treatment of fibrotic disease. J Pathol. 2013;231(3):273–89.
20. Cui L, Lu Y, Zheng J, Guo B, Zhao X. ACTN1 promotes HNSCC tumorigenesis and cisplatin resistance by enhancing MYH9-dependent degradation of GSK-3β and integrin β1-mediated phosphorylation of FAK. J Exp Clin Cancer Res. 2023;42(1):335.
21. Chen Q, Zhou XW, Zhang AJ, He K. Correction to: ACTN1 supports tumor growth by inhibiting Hippo signaling in hepatocellular carcinoma. J Exp Clin Cancer Res. 2021;40(1):128.
22. Faleschini M, Melazzini F, Marconi C, Giangregorio T, Pippucci T, Cigalini E, Pecci A, Bottega R, Ramenghi U, Siitonen T, et al. ACTN1 mutations lead to a

benign form of platelet macrocytosis not always associated with thrombocytopenia. Br J Haematol. 2018;183(2):276–88.
23. Liu Z, Wang Y, Dou C, Xu M, Sun L, Wang L, Yao B, Li Q, Yang W, Tu K, et al. Erratum: Hypoxia-induced up-regulation of VASP promotes invasiveness and metastasis of hepatocellular carcinoma: Erratum. Theranostics. 2023;13(3):910–2.
24. Holt MR, Critchley DR, Brindle NP. The focal adhesion phosphoprotein, VASP. Int J Biochem Cell Biol. 1998;30(3):307–11.
25. Nast-Kolb T, Bleicher P, Payr M, Bausch AR. VASP localization to lipid bilayers induces polymerization driven actin bundle formation. Mol Biol Cell. 2022;33(10):ar91.

Publisher's note